ALICE/2000-17
Internal note/ T0
14 June 2000

BEAM TESTS OF THE SECOND PROTOTYPE OF A CHERENKOV COUNTER FOR THE ALICE T0 DETECTOR

V.A.Grigoriev,V.A.Kaplin, A.I.Karakash, V.A.Loginov, A.L.Rakhmanov
Moscow Engineering Physics Institute

A.B.Kurepin, A.I.Maevskaia, V.I.Rasin, A.I.Reshetin
Institute for Nuclear Research, Russian Academy of Sciences, Moscow

A.V.Akindinov, A.N.Martemianov, V.A.Sheinkman, A.V.Smirnitsky
Institute for Theoretical and Experimental Physics, Moscow

ABSTRACT

The second prototype of a Cherenkov counter consisting of a quartz radiator (cylinder 26 mm in diameter, 30 mm long) and a PMT Hamamatsu R3432-01 has been tested in a 1.28 GeV/c pion beam. A constant fraction discriminator EG&G was used at the output of the PMT. Measurements in a beam with a limited cross-section 0.8 x 0.8 cm^2 gave a 50 ps time resolution of the detector. In a “broad-beam” geometry the time resolution of the detector was measured to be 55 ps. In both cases an off-line correction was used due to inadequate characteristics of the CFD, confirmed by the measurements at laboratory conditions using a pulsed laser. Another type of a CFD (4000M) properly adjusted using a pulsed laser and optical filters provided a 55 ps resolution in a “broad-beam” geometry without any off-line correction. Monte-Carlo simulations of p-p collisions show, that an averaging procedure for the signals coming from the two arrays of the T0 detector significantly improves the time resolution for the T0 signal. At a 50 ps resolution of each array, the resulting resolution for the T0 signal is equal to 40 ps the fluctuation of the vertex position and of the particles’ velocities being taken into account.

1.INTRODUCTION

In our previous ALICE Internal note [1] we presented the results of the beam tests of the first prototype of a Cherenkov counter for the ALICE T0 detector. The first prototype consisted of a PMT Hamamatsu R3432-01 and a quartz radiator 25 x 30 x 12 mm ^{3}. In our tests we used the ITEP test beam facility and a leading edge discriminator at the output of the Cherenkov detector. The cross-section of the beam was limited to 0.8 x 0.8 cm^2 by two additional scintillation counters. The main result of that test was as follows: a 48 ps resolution (sigma) in a wide dynamic range of a PMT High Voltage (1100 – 2400 V). As we used a leading edge discriminator, a 48 ps resolution was obtained after an off-line correction.

The main goal of our R&D still remains to achieve a 50 ps resolution of the detector "on-line", i.e. without any off-line correction for a real geometry of the detector – a cylindrical 3 cm thick quartz radiator having the diameter equal to the diameter of the PMT (26 mm) . In this paper we describe the experimental results obtained in a real geometry, as well as the results of some studies of the first prototype of a constant fraction discriminator (CFD), which should be used in the T0 detector in order to obtain good time resolution for the T0 signal "on-line" in a wide dynamic range of PMT amplitudes.

2. MONTE-CARLO SIMULATIONS OF THE TIME RESOLUTION AND THE VERTEX POSITION DETERMINATION FOR A 50 ps RESOLUTION OF A CHERENKOV COUNTER

Although a 50 ps resolution of the first prototype of a Cherenkov counter was obtained under rather favorable conditions of the experiment, which provided for a good light collection efficiency, one can expect that the same resolution can be achieved for a practical geometry of the counter in a wide beam. The main reason for this assumption is that in laboratory conditions using a well adjusted CFD and a pulsed laser the time resolution obtained for the same number of photoelectrons as in beam tests was about 35-40 ps[1]. We conclude therefore that the contribution of the electronics used in the beam tests was rather significant, so that its optimization can improve the time resolution of the counter. That is why in our Monte-Carlo simulations we assumed that each array of the Cherenkov counters had a 50 ps time resolution.

Monte-Carlo simulations were carried out at CERN by our group using ALIROOT 3.03. The geometry of the T0 detector was slightly changed, namely each PMT was aligned along the central particle's trajectory coming from the center of the vertex, thus corresponding to the last option of the detector with 12 PMTs in each array. Fig.1 gives the multiplicity distribution of events generated by PYTHIA for p-p collisions. The geometrical efficiency for non-diffractive processes is 87%. Fig.2 gives the arrival time difference $t_{left} - t_{right}$ (a) and the average arrival time $(t_{left} + t_{right})/2$ (b) for the first arriving particles for a fixed vertex position. The finite widths of the distributions of 35 ps and of 17 ps correspondingly are due to the variations of the velocities of the arriving particles. Fig.3(a) gives the arriving time difference $t_{left} – t_{right}$ assuming that each array has a finite time resolution, described by a Gaussian with sigma = 50 ps. The variations of the particles' velocities were also taken into account. The time resolution in this case is about 80 ps, which brings to a 23 mm (sigma) resolution of the position of the vertex (Fig.3,b).

The T0 signal distribution calculated for a 50 ps resolution of each array is shown in Fig.4. The variations of particles' velocities (Fig.2, b) were also taken into account. The time resolution for T0 taken as ($t_{left} + t_{right}$)/2 is equal to 38 ps, i.e. it is better than the time resolution of each array, as expected.

In the second run of simulations the spread of the vertex position with sigma = 5.6 cm was also taken into account, as well as a 50 ps time resolution of each detector array. The calculations of the geometrical efficiency of registration in p-p collisions for the non-diffractive processes gave the value: 88%. Using the simulated arrival times for each event in each array as experimental data, all other distributions were reconstructed using an event reconstruction subroutine. Fig.5 gives the reconstructed distribution of time difference between left and right arrays. Fig.6 gives the reconstructed distribution of the position of the vertex with RMS 5.56 cm. Simple calculations give sigma = 6 cm. The discrepancy is rather due to poor statistics. Anyway the 50 ps resolution of each T0 detector array does not broaden significantly the collision region, taken as 3σ.

3. PRINCIPAL RESULTS OF BEAM TESTS OF THE CHERENKOV DETECTOR PROTOTYPE.

For the second prototype of a Cherenkov detector we used a cylindrical quartz radiator 3 cm long with a diameter equal to the PMT diameter (26 mm) and the same PMT R3432-01, as in our previous tests [1]. The optical contact was provided by optical grease. In our test runs we used the same beam facility of ITEP as described in [1]. The start detector like in previous tests consisted of two identical S1 and S2 scintillation counters. The time resolution of the START detector was taken as the TOF resolution between S1 and S2 divided by $\sqrt{2}$. The only difference from the previous tests was that the signal coming from the Cherenkov detector was fed to a free input of the CFD EG&G of the same facility without any special adjustment. The pions of 1.28 GeV/c momentum were identified by a supplementary TOF system of the facility.

The runs were made at two different conditions. In the first set of runs we used the supplementary detectors limiting the cross-section of the beam to 0.8 x 0.8 cm^2. The typical result is given in Fig.7. Fig.7(a) gives the two-dimensional distribution of the TOF data between S1 and the Cherenkov detector. It is clearly seen that the CFD did not operate properly. The experimental data therefore were fitted by a straight line giving a shift of the TOF distribution of about 100 ps/ 100 QDC channels. Fig.7(b) gives the result of this fit. The off-line corrected data were fitted by a Gaussian (Fig.7c). The TOF S1-S2 data were also fitted by a Gaussian (Fig.7d). The resulting value of the time resolution of the Cherenkov detector was estimated from this data to be equal to 50 ps at 100% physical efficiency.

In the second set of runs similar measurements were made in a “broad-beam” geometry, the beam defining detectors being switched off. The typical results are given in Fig.8, and they are quite similar to those given in Fig.7. The time resolution after off-line correction was 55 ps. The physical efficiency in this case was 97%. 3% of pulses with small amplitudes (edge effects) registered by a QDC were cut by the threshold of the CFD.

Since the characteristics of the EG&G CFD looked rather abnormal, we made detailed laboratory studies of this CFD using the same PMT and a pulsed laser. The amplitudes of the output signals of the PMT were varied using optical filters. The results of these measurements are shown in Fig.9. Fig 9(a) gives the delay of the output signal of the EG&G as a function of the input amplitude. Since the detector amplitudes in our measurements were below 1V, Fig 9(b) gives the part of EG&G characteristics below 1V. A fit by a straight line gives an average shift of the delay about 100 ps/ 100 QDC channels corresponding to the data of the beam tests. It is visible from Fig.9(b) that the linear fits of the experimental data shown in Fig.7 and Fig.8 are very poor, and hence the values of time resolution obtained in these runs are somewhat worse than they could be.

The experimental results given in this section clearly show that in order to obtain a 50 ps resolution ‘on-line’ in a wide dynamic range of the PMT output signals, the front-end electronics, mainly the CFD, should be optimized for a given type of detector.

4. SOME PRELIMINARY RESULTS OF THE OPTIMISATION OF A CFD.

We consider two possible options for the front-end electronics of the T0 detector: a) preliminary summation of the PMT signals by 1 or more adders in each array (Fig.10.a) , b) individual CFD for each PMT (Fig.10.b). Independently of the final choice there are some crucial elements common for both options. First of all the delays of the signals coming from each PMT of an array should be made equal with the precision about 10 ps. It is possible to do so by changing the value of the HV of a PMT. Fig.11(a) gives the delay of the PMT signal as a function of the HV. The Dubna HV supply we intend to use has a HV instability of 0.05%, which means +- 1V for 2000 V. So it is possible to make a precise equalizing of the delays by slightly varying the HV without large changes of the PMT amplitude (Fig.11.b).

In both options the signals were fed into a time-to-coordinate compensator. It is a well-known device, since its construction is based on the same principles as time-to-amplitude converters or double threshold discriminators [2,3], which intrinsic resolution can be as good as 10 ps, it seems quite feasible to achieve a 20 ps resolution, needed in our case for a device based on modern electronic components.

From our point of view the most crucial element is a CFD. The conventional industrial CFDs usually have a +- 25 ps variations of the delay of the output signal over a wide dynamic range (1:100). Our experience shows that this characteristic is not confirmed for a real pulse shape of the PMT R3432-01. For our studies we took a slightly modified CFD4000, produced in our laboratory. The first tests with a pulse generator reproducing the pulse shape of the PMT showed that one can easily obtain the characteristics mentioned above. Still the characteristics obtained with a real signal (PMT + pulsed laser) differ greatly from those obtained with a pulse generator. Therefore all our studies described below were made with the same PMT we used in beam tests and a pulsed laser (500 ps FWHM). At first the amplitude at the output of the PMT was fixed, and the CFD input signal was varied using a compensated RC attenuator at the input of the CFD. Fig.12 gives the variations of the delay of the CFD as a function of the amplitude of the input signal for different values of the adjustment delay, given by length of the delay cable (50 ps/cm) in logarithmic (a) and linear (b) scales. One can see that it is possible to achieve output delay variations +- 20 ps in the dynamic range 1:100 (e.g. l = 10 cm), which seems quite satisfactory for our purposes. However when we used optical filters for the signal attenuation instead of the RC attenuator, the characteristics appeared to be rather different from those given in Fig.12, and a special precise adjustment of the CFD using the optical filters was applied to improve them. Fig.13 gives the CFD characteristics after this adjustment at l=10 cm in linear (a) and logarithmic (b) scales. Rhombs give the CFD characteristics measured with optical filters. Squares give the characteristics of the CFD measured with the RC attenuator after adjustment with optical filters.

The CFD 4000M adjusted with optical filters as shown in Fig.13 was used in a beam test (pions, 1.28 GeV/c) in a “wide-beam” geometry. The results of this test are shown in Fig.14. One can see that the two-dimensional TOF distribution looks now quite parallel to the amplitude axis, the time resolution calculated without any off-line correction is practically the same as in the previous test (56 ps). The amplitude distribution for pions is given in Fig15, and it is very similar to that obtained by the Japanese Hiroshima group in [4].

5. CONCLUSIONS.

- Our experimental results show, that a 50 ps resolution of a Cherenkov detector with a 3 cm thick cylinder radiator for minimum ionizing particles is feasible. Even already achieved experimental value of 55 ps for a “broad-beam” geometry seems quite satisfactory since the averaging of two signal’s time intervals for the left and right arrays gives a time resolution of the T0 signal about 43 ps. This value includes σ = 17 ps of the particles velocities deviations. A resolution of 25 ps of an averaging compensator will bring to the resulting 50 ps resolution for the T0 signal. Still we do not think that the 55 ps resolution we have now is a practical limit. We believe that the contribution of electronics to the resolution in our experimental conditions was rather large and that it can be decreased by optimization. The other way is to utilize the U.V. part of the Cherenkov emission, but in fact we do not think it would be really necessary.
- To our mind the main problem which should be solved is an adequate front-end electronics, especially constant fraction discriminators. Our first attempt to modify slightly the popular CFD4000 and adjust it properly shows that it is quite feasible to have a CFD with +-20 ps delay time deviations over a dynamic range of the input signals 1:100 or so.
- It is also obvious that in order to achieve the proper characteristics of the front-end electronics one should use a real signal coming from a PMT.
- The possibility to use a pulsed laser instead of a particle beam is a serious advantage of the design. Really, using a pulsed laser and optical filters it is possible to reproduce more or less adequately the experimental conditions of p-p, Ca-Ca and Pb-Pb runs. It makes also possible to adjust the whole electronic set-up, to equalize the delays, etc., which is a very important stage of work for a multi-element system.
- The specific feature of a Cherenkov detector is that it is directional and thus insensitive to the backsplash particles ,coming from the absorber.

REFERENCES.

1. V.A.Grigoriev, et al. Beam tests of the first prototype of a Cherenkov counter for ALICE T0 detector. ALICE/2000-05, Internal note/trigger, 14 March 2000.
2. L.Ondrish, S.V.Muhin, S.B.Rihvitsky, et al., Preprint JINR,HEL, P 13-5373, Dubna,1970.
3. Rothermel H. Compensated time-of flight telescope for spaceborn cosmic ray measurements. IEEE Trans.Nucl.Sci.,1977,V.NS-24, Nr.1, p 801-803.
4. K.Ikematsu, et al. A start timing detector for the collider experiment PHENIX at RHIC-BNL. Nuclear Instr. and Meth., A411,(1988),p238-248.

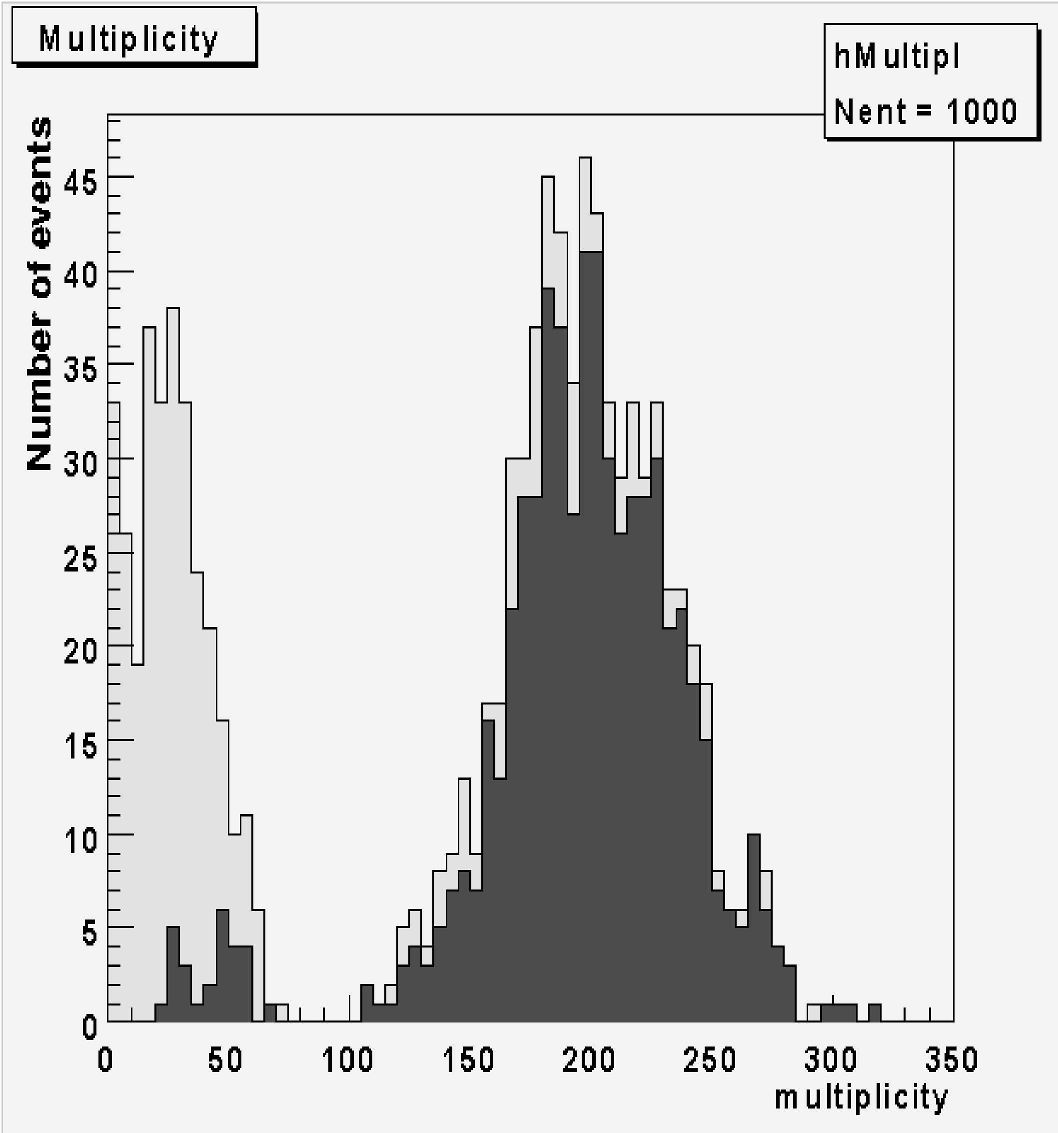

Fig. 1. The multiplicity distribution in p-p collisions.

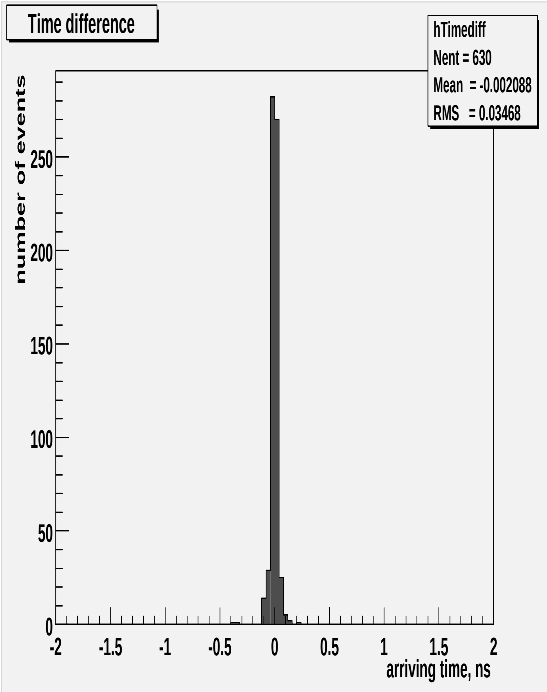

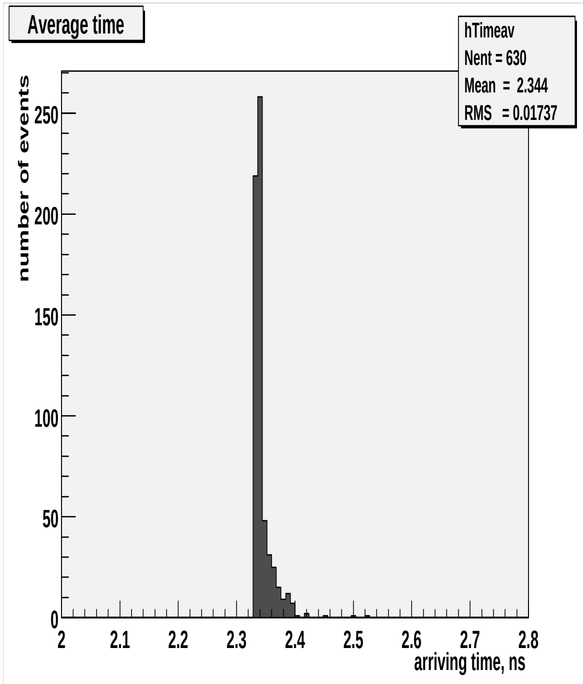

Fig.2a. Arriving time difference distribution for left and right arrays.

Fig.2b. Average arriving time distribution for both arrays.

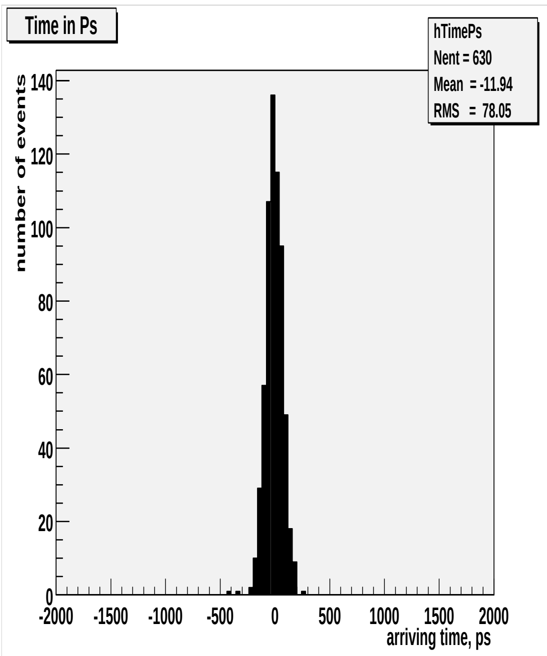

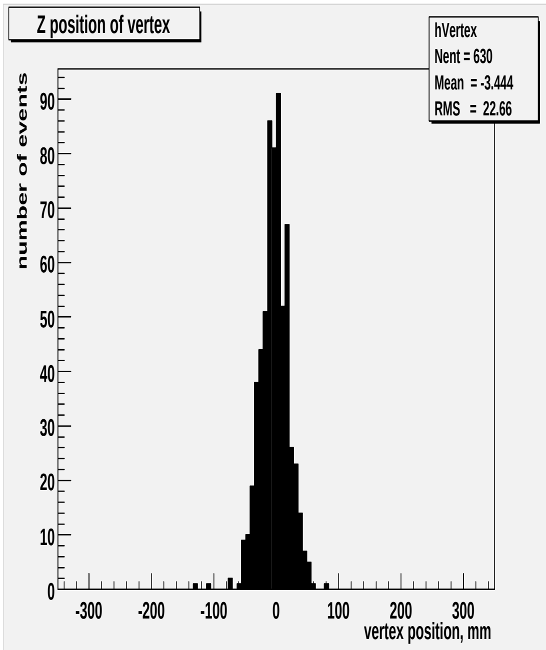

Fig.3a. Arriving time difference distribution for left and right arrays for 50ps resolution of each array.

Fig.3b. Vertex position distribution reconstructed using time difference distribution given in Fig3a.

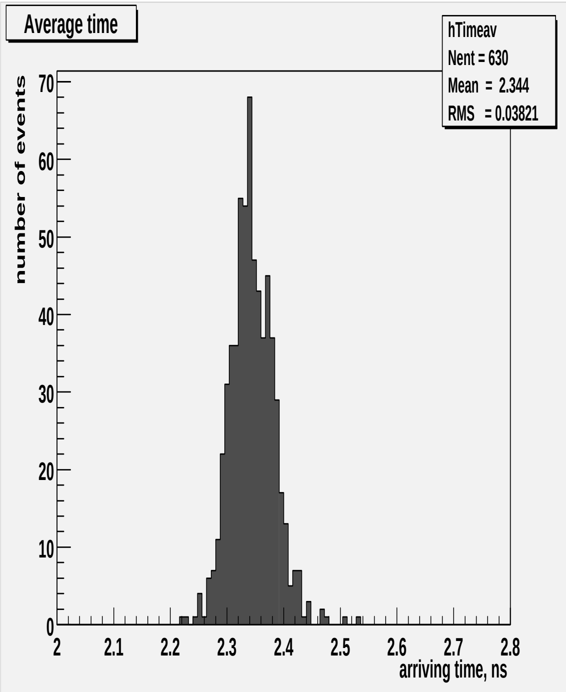

Fig . 4 Average arrival time distribution (T0 signal) for 50ps time resolution of each Cherenkov counter array

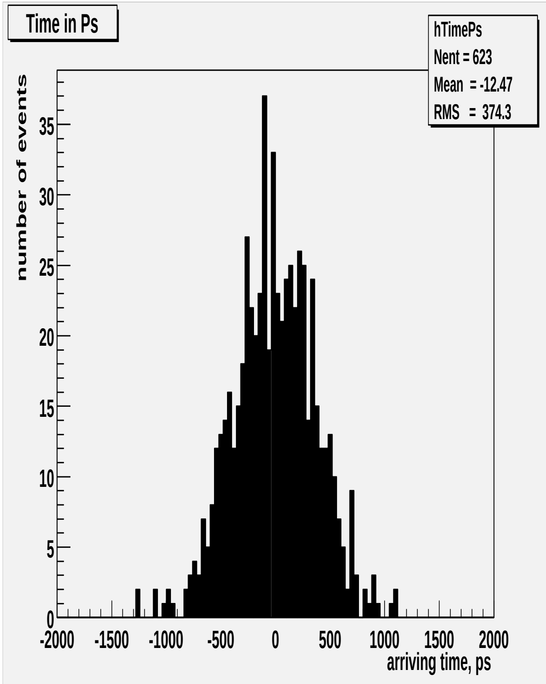

Fig.5. The reconstructed time difference with initial σ_{vertex}=5.6cm and σ_{det} =50ps(of each array)

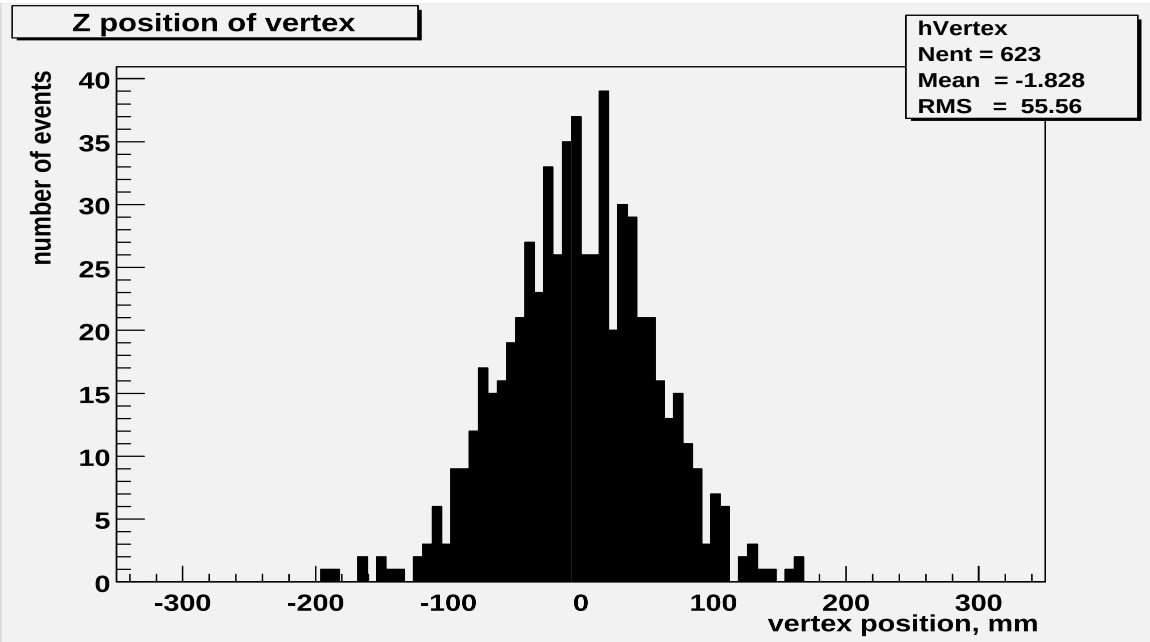

Fig.6. The reconstructed position of the vertex with initial σ_{vertex}=5.6cm and σ_{det} =50ps(of each array)

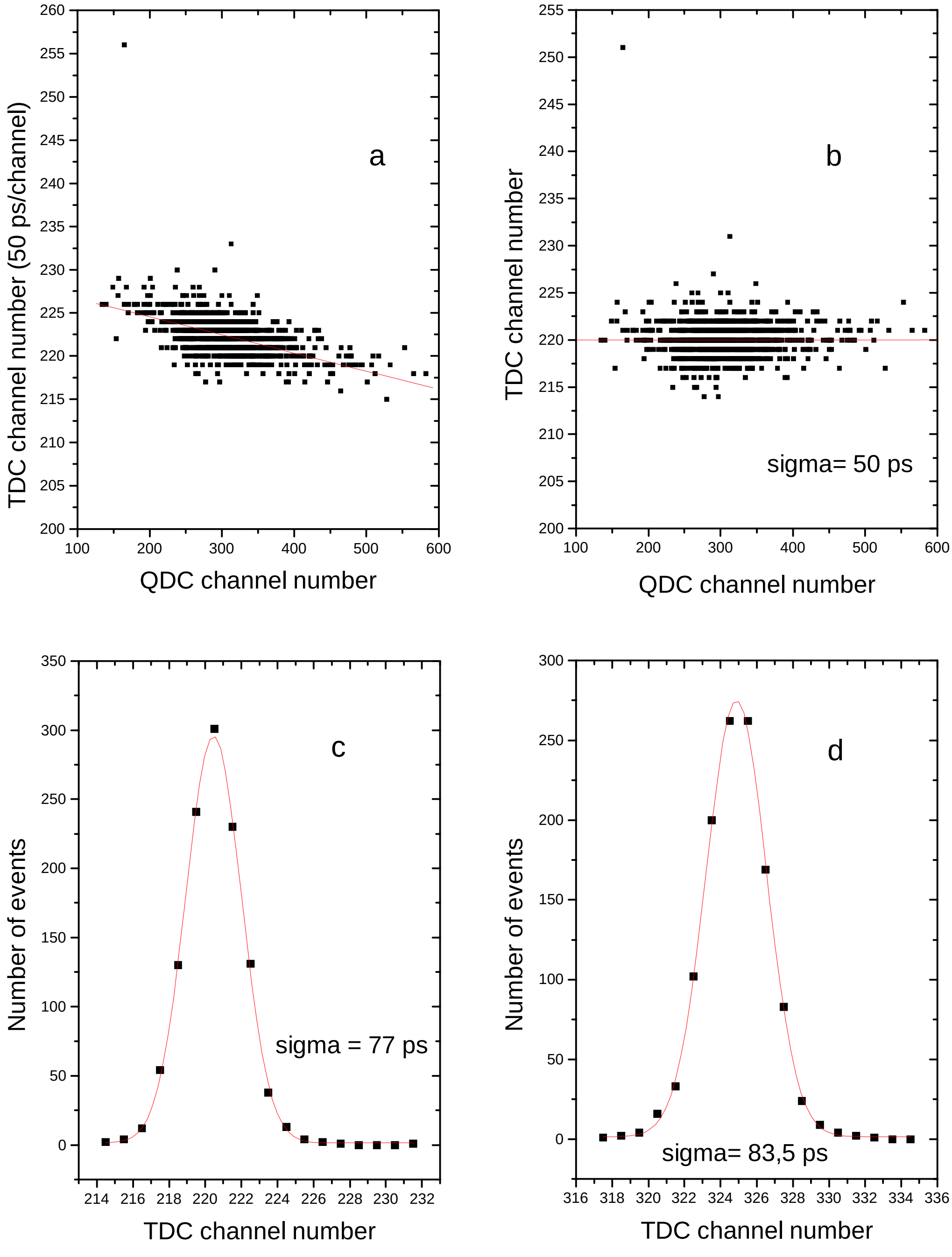

Fig. 7. a) raw data of TOF two-dimensional distribution between start detector and Cherenkov detector with 0,8X0.8 cm^2 pions beam;

b) corrected TOF data;

c) Gaussian fit of corrected TOF data;

d) Gaussian fit of S_1-S_2 TOF data.

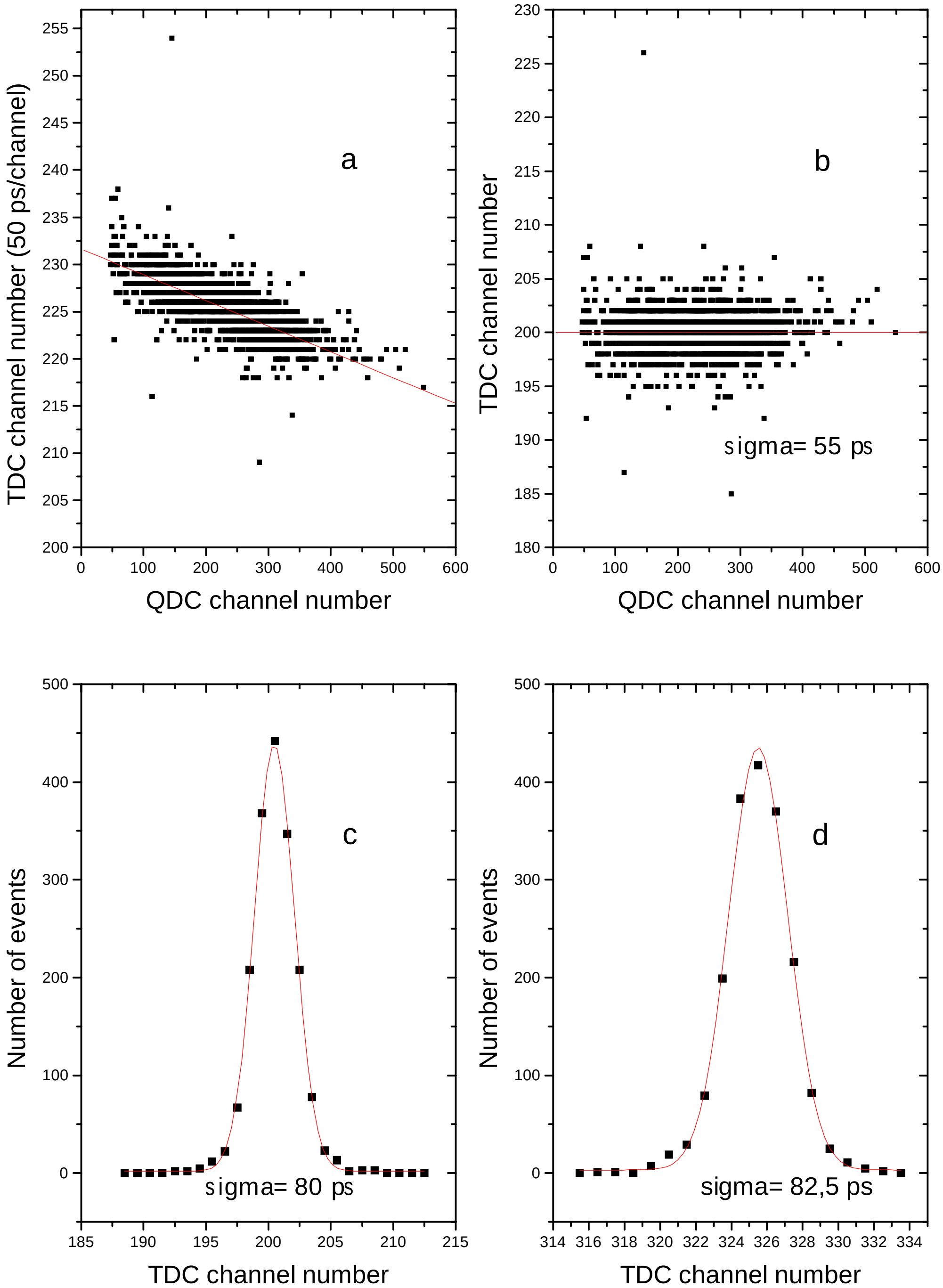

Fig. 8. a) rawdata of TOF two-dimensional distribution between Cherenkov detector and start detector in a broad beam;

b) corrected TOF data;
c) Gaussian fit of corrected TOF data;
d) Gaussian fit of S_1-S_2 TOF data.

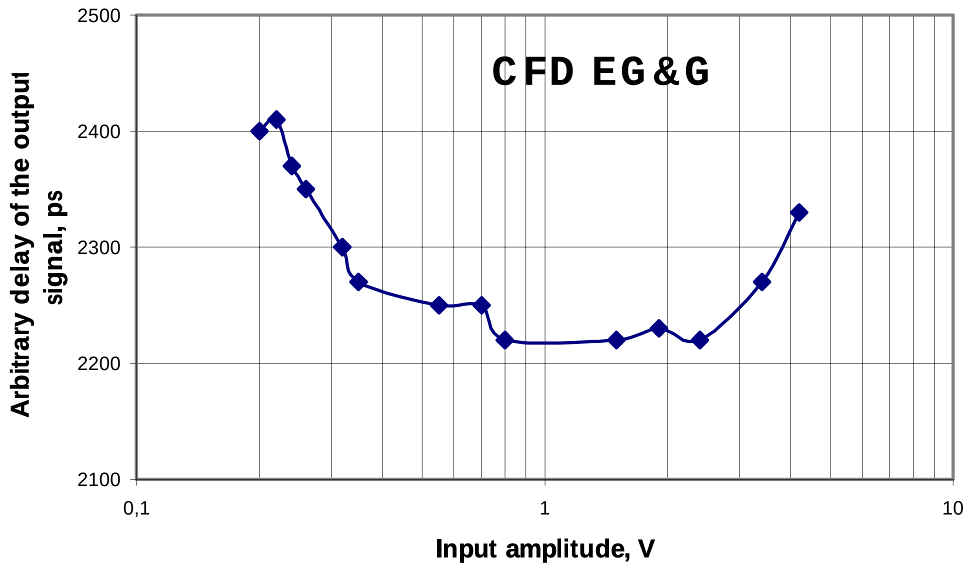

a

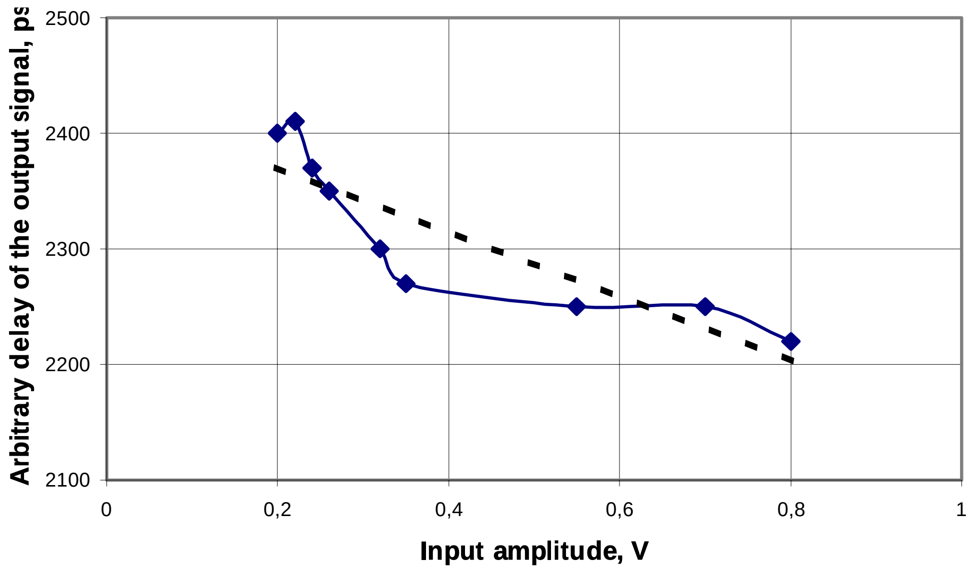

b

Fig. 9 a) The output signal delay of the CFD as a function of the input signal amplitude;
b) The part of the characteristics below 1 V of the input amplitude

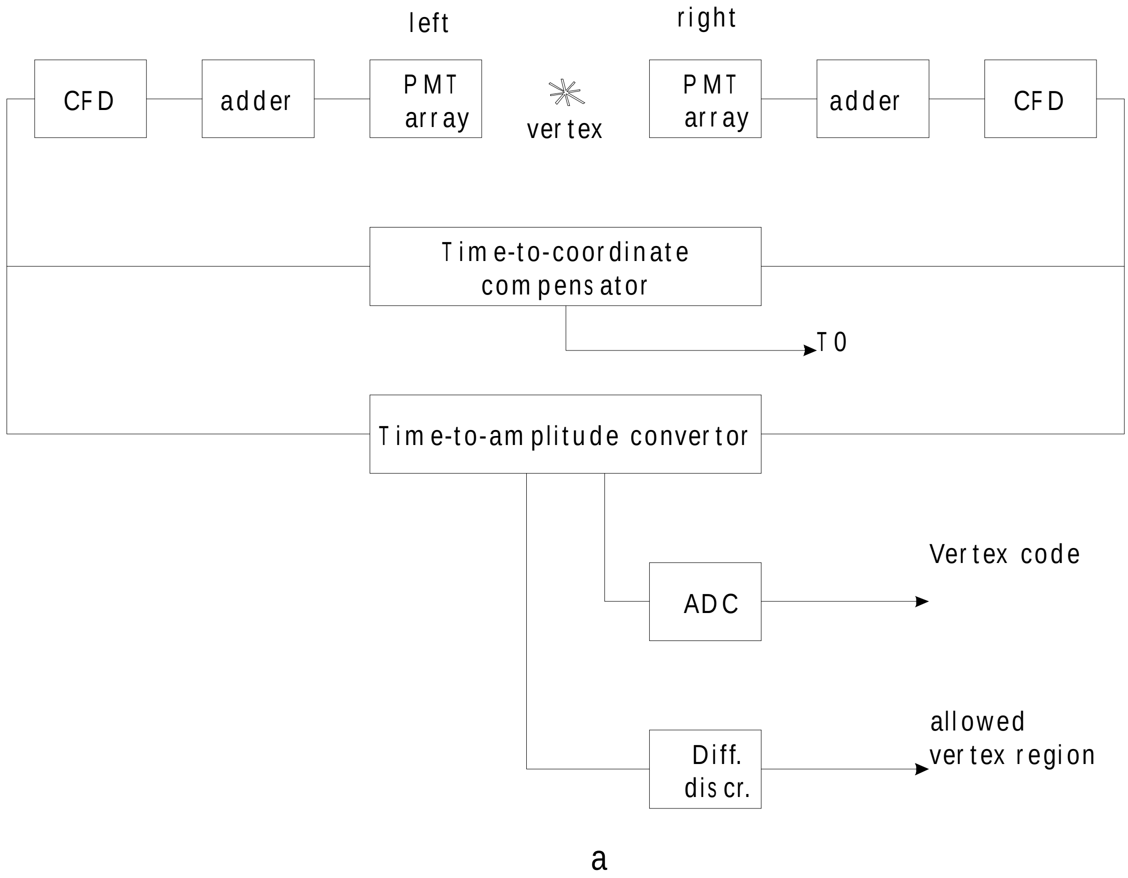

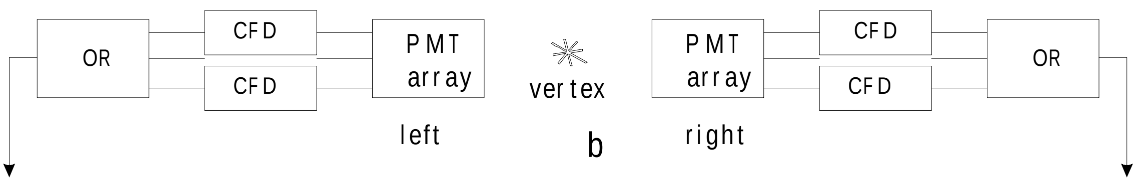

Fig. 10. Simplified layout the front-end electronics
a) with preliminary summation of PMT's signals;
b) with an individual CFD for each PMT.

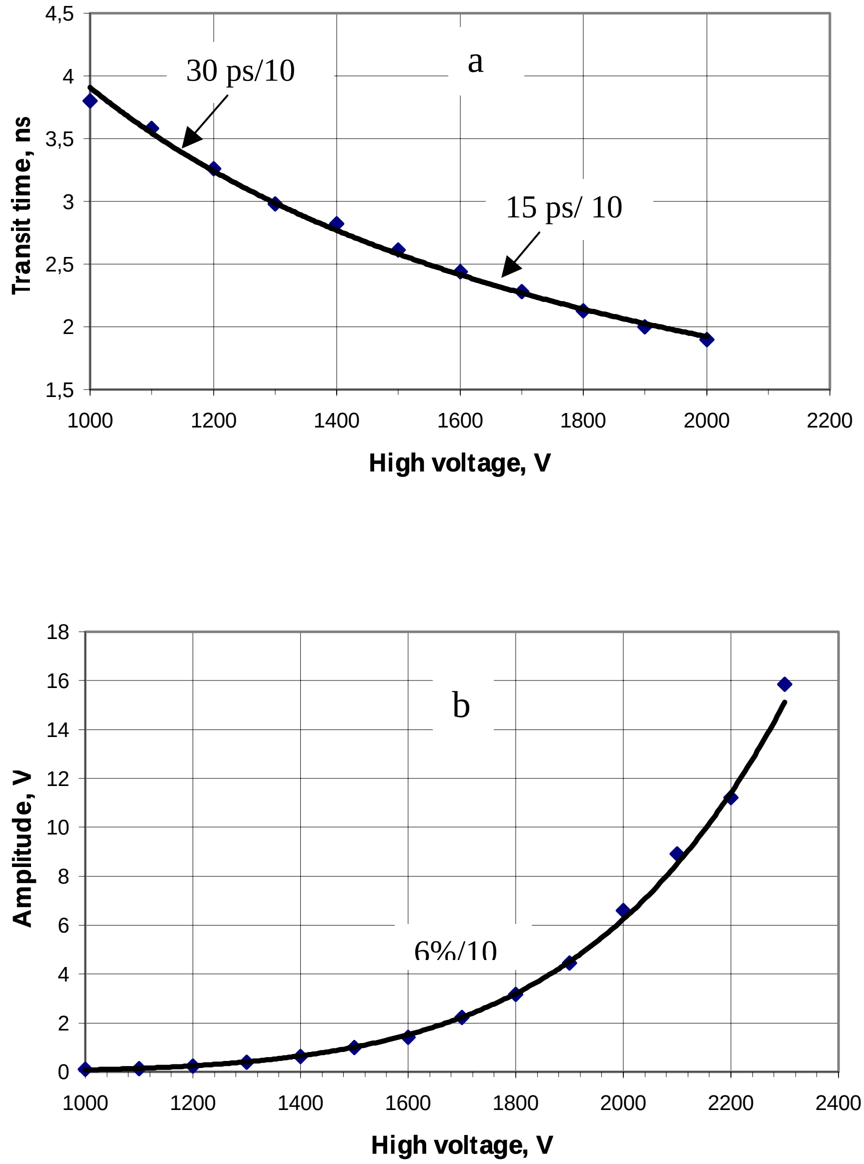

Fig.11. a) PMT signal delay as a function of the high voltage;
b) PMT output amplitude as a function of the high voltage.

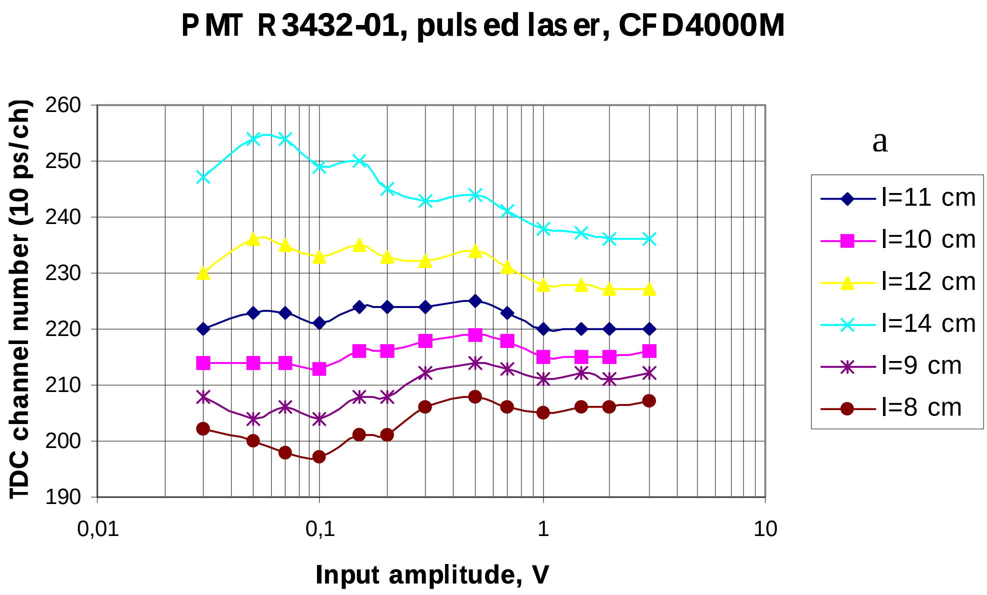

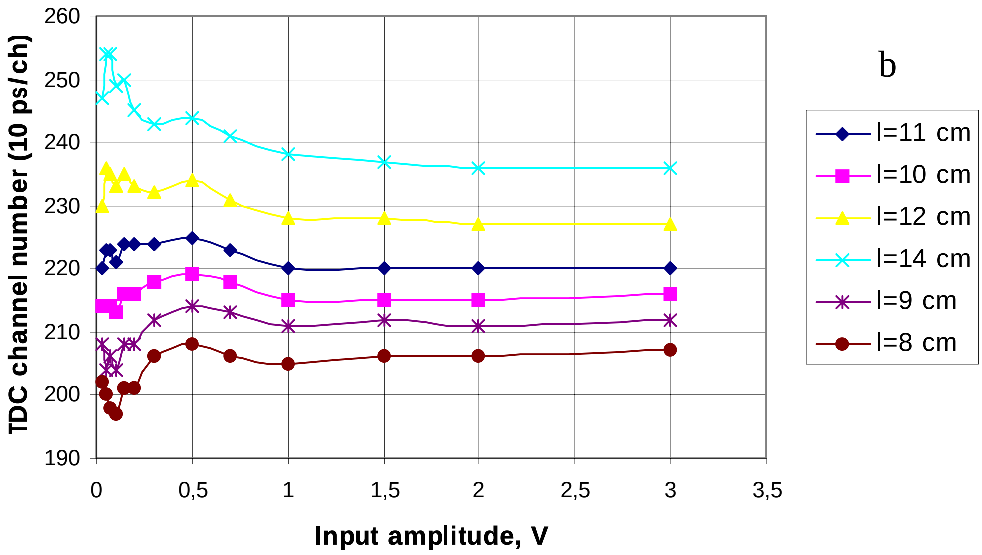

Fig. 12. The variation of the delay of the CFD output signal as a function of the of the input signal at different input delay l (50 ps/cm). The amplitude of the CFD input signal was varied using a compensated RC-attenuator at a constant PMT output signal.

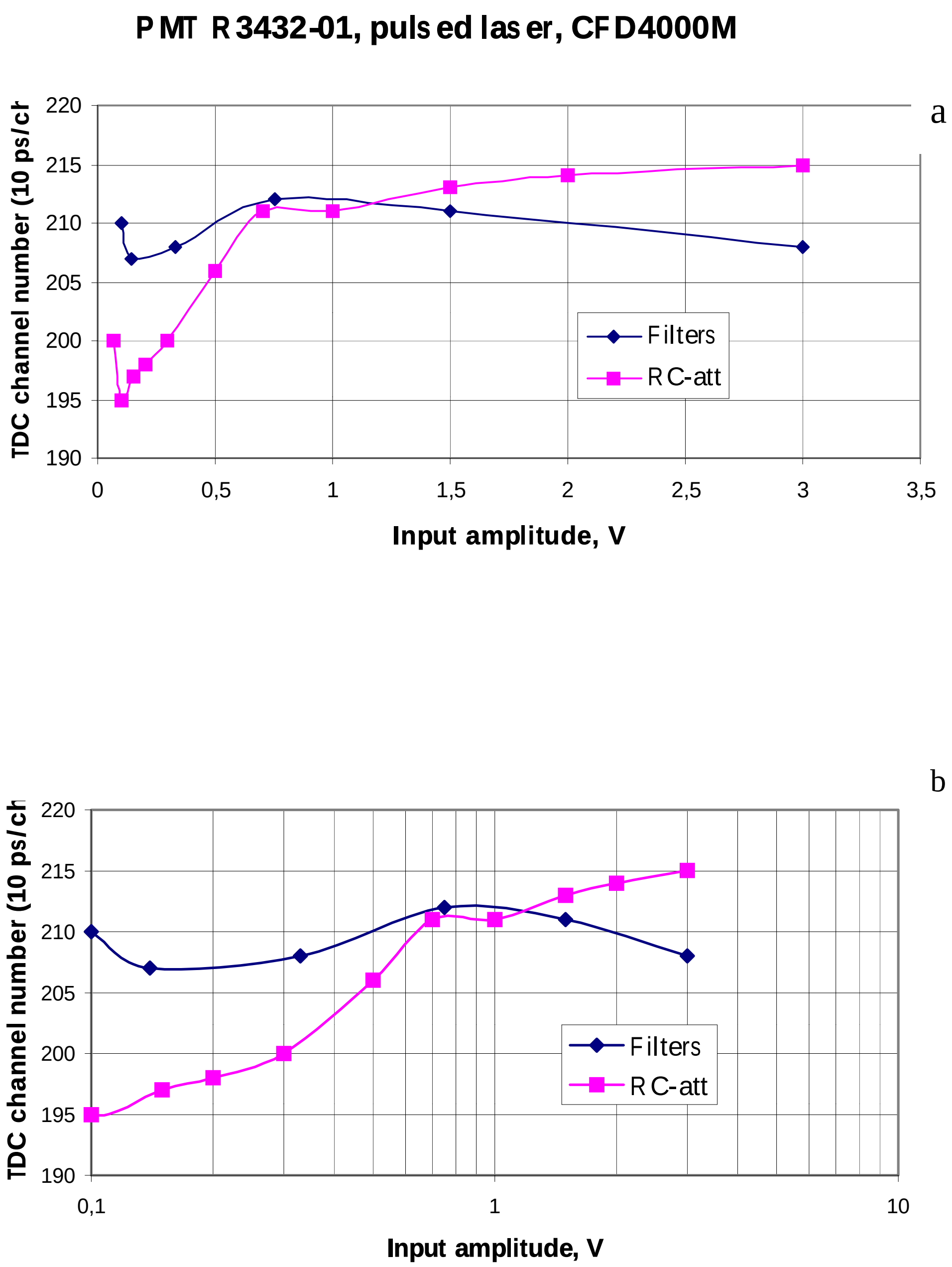

Fig. 13. The variation of the delay of the CFD output signal as a function of the amplitude of the input signal after adjustment with optical filters.
Rhombs – the results of the adjustment with optical filters;
Squares – measurements with RC-attenuator.

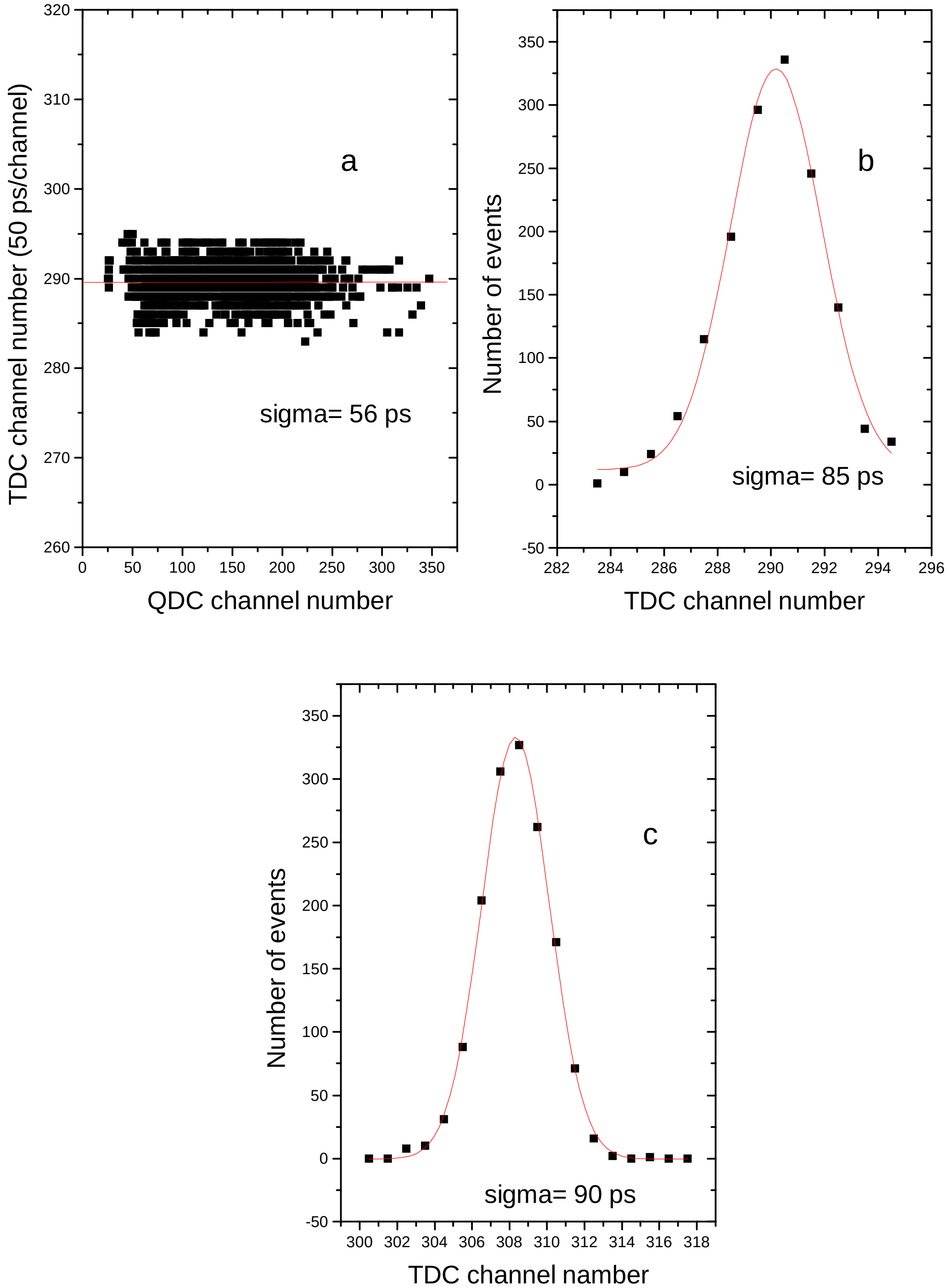

Fig. 14.a) Two-dimensional TOF distribution between Cherenkov detector and start detector in a broad beam;

b) Gaussian fit of TOF data;

c) Gaussian fit of S_1-S_2 TOF data.

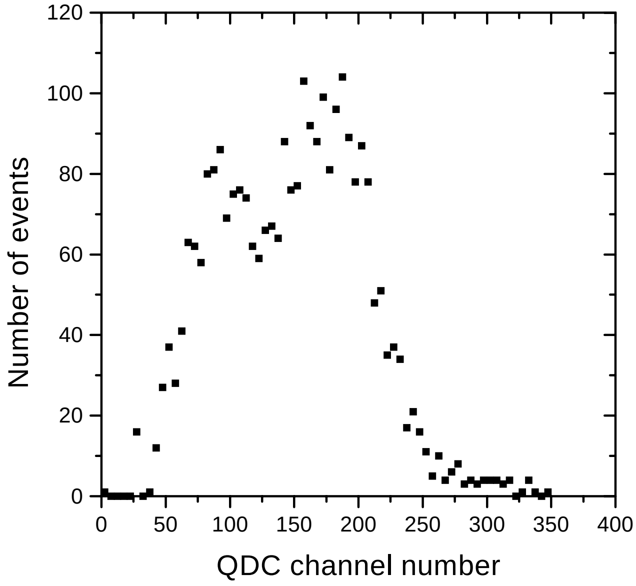

Fig. 15. Amplitude spectrum of the Cherenkov detector for pions 1,28 GeV/c for the “broad-beam” geometry.